Syntaxin 5 regulates the endoplasmic reticulum channel-release properties of polycystin-2

Lin Geng[†], Wolfgang Boehmerle[‡], Yoshiko Maeda[†], Dayne Y. Okuhara[†], Xin Tian[†], Zhiheng Yu[†], Chi-un Choe[‡], Georgia I. Anyatonwu[‡], Barbara E. Ehrlich[‡], and Stefan Somlo[†§¶]

Departments of [†]Internal Medicine, [‡]Pharmacology, and [§]Genetics, Yale University School of Medicine, New Haven, CT 06510

Edited by David E. Clapham, Harvard Medical School, Boston, MA, and accepted by the Editorial Board August 6, 2008 (received for review May 30, 2008)

Polycystin-2 (PC2), the gene product of one of two genes mutated in dominant polycystic kidney disease, is a member of the transient receptor potential cation channel family and can function as intracellular calcium (Ca^{2+}) release channel. We performed a yeast two-hybrid screen by using the NH_2 terminus of PC2 and identified syntaxin-5 (Stx5) as a putative interacting partner. Coimmunoprecipitation studies in cell lines and kidney tissues confirmed interaction of PC2 with Stx5 *in vivo*. *In vitro* binding assays showed that the interaction between Stx5 and PC2 is direct and defined the respective interaction domains as the t-SNARE region of Stx5 and amino acids 5 to 72 of PC2. Single channel studies showed that interaction with Stx5 specifically reduces PC2 channel activity. Epithelial cells overexpressing mutant PC2 that does not bind Stx5 had increased baseline cytosolic Ca^{2+} levels, decreased endoplasmic reticulum (ER) Ca^{2+} stores, and reduced Ca^{2+} release from ER stores in response to vasopressin stimulation. Cells lacking PC2 altogether had reduced cytosolic Ca^{2+} levels. Our data suggest that PC2 in the ER plays a role in cellular Ca^{2+} homeostasis and that Stx5 functions to inactivate PC2 and prevent leaking of Ca^{2+} from ER stores. Modulation of the PC2/Stx5 interaction may be a useful target for impacting dysregulated intracellular Ca^{2+} signaling associated with polycystic kidney disease.

Ca^{2+} channel | polycystic kidney disease | t-SNARE | TRP channel

Autosomal dominant polycystic kidney disease (ADPKD) is characterized by the growth of cysts, occurring over decades, in previously normal appearing kidney tubules (1). A functional hallmark of ADPKD is the loss of a calcium (Ca^{2+}) signal that serves to inhibit dysregulated kidney tubule cell proliferation, polarization, and secretory function. Either of two causative genes, *PKD1* or *PKD2*, can initiate cyst formation after homozygous loss-of-function mutations, typically resulting from a combination of germline mutation on one allele followed by somatic second step mutation occurring at the level of individual cells. The respective protein products, polycystin-1 (PC1) and polycystin-2 (PC2), form a receptor-channel complex in the membrane of the apical primary cilia in renal tubular cells (2, 3), as well as in bile and pancreatic duct cells. PC2 (TRPP2), a member of the transient receptor potential (TRP) cation channel family, is abundantly expressed in the endoplasmic reticulum (ER) membrane (4) and has been shown to function as a Ca^{2+} release channel from intracellular stores (5, 6). Indirect evidence has led to the proposal that PC2 channel activity is required for the rise in cellular Ca^{2+} in ciliated monolayers of cultured epithelial cells under conditions of laminar shear stress because of fluid flow (7, 8). This response to flow requires Ca^{2+} from both extracellular and ER stores (9).

Although variations in the reported channel properties of PC2 exist, it is generally accepted that PC2 is a high conductance cation channel (40–177 pS) whose activity is modulated by Ca^{2+}, pH (10), and phosphorylation (11). Maintenance of cellular Ca^{2+} homeostasis within tight tolerances requires exquisite regulation of PC2 activity, especially in the ER, where PC2 is abundantly expressed (5). PC2 functionally interacts with both major types of intracellular release channels, $InsP_3R$ (6) and RyR (12), to modulate intracellular Ca^{2+} signaling. However, neither $InsP_3R$ nor RyR directly regulate PC2 channel activity (6, 12). Among other PC2 interacting proteins described to date, only PC1, α-actinin, mammalian diaphanous-related formin 1 (mDia), and fibrocystin have been suggested to modulate PC2 channel activity (13–16). However, interaction with PC1, α-actinin, and fibrocystin have been proposed to activate the PC2 channel (13, 14, 16), and mDia1 does not act at the ER (17), leaving unanswered the question of how the PC2 channel is kept inactive at the ER membrane.

We performed a yeast two-hybrid screen by using the NH_2 terminus of PC2 and among the candidate interacting partners we identified was syntaxin-5 (Stx5). Syntaxins are a large family of proteins with well-defined functions in vesicle targeting and fusion. In addition, syntaxins have been shown to interact with, and regulate the channel activity of, a number of transport proteins, most prominently the synaptic *N*- and P/Q-type Ca^{2+} channels (18), but also Kv channels (19), CFTR (20), and ENaC (21). The various syntaxins localize to specific membrane domains within the cell. Stx5 is an ER- and Golgi-associated t-SNARE. Stx5 function is essential for formation of ER-derived transport vesicles and for delivery of cargo to the Golgi (22), as well as for intra-compartment fusion in the vesicle-tubular compartment and *cis*-Golgi cisternae formation (23). The *in vivo* interaction of PC2 with Stx5 was confirmed by coimmunoprecipitation studies including native kidney tissue. The region of physical interaction was defined as the t-SNARE domain of Stx5 and amino acids 5 to 72 of PC2. Single channel analyses of PC2 function *in vitro* showed that the interaction with Stx5 specifically inactivates channel activity in a concentration dependent manner. *In vivo* studies examining Ca^{2+} dynamics in epithelial cells in culture showed that expression of a mutant form of PC2 that cannot bind Stx5 results in increased baseline cytosolic Ca^{2+} levels, with concomitant decrease in ER Ca^{2+} stores and reduced ER Ca^{2+} store release in response to arginine vasopressin (AVP) stimulation. In aggregate, the data show that PC2 in the ER plays a role in cellular Ca^{2+} homeostasis and that Stx5 functions to inactivate PC2 and prevent leak of Ca^{2+} from ER stores.

Results

PC2 Coimmunoprecipitates with Stx5 in Cells and Tissues. Stx5 was identified as a putative PC2 interacting protein in a yeast two-hybrid screen by using the cytoplasmic NH_2-terminal domain of PC2 (amino acids 3–213) as bait. Stx5 is translated from a single

Author contributions: L.G., W.B., B.E.E., and S.S. designed research; L.G., W.B., Y.M., D.Y.O., X.T., Z.Y., C.C., and G.I.A. performed research; W.B., C.C., B.E.E., and S.S. analyzed data; and S.S. wrote the paper.

The authors declare no conflict of interest.

This article is a PNAS Direct Submission.

¶To whom correspondence should be addressed at: Section of Nephrology, Yale University School of Medicine, P.O. Box 208029, 333 Cedar Street, New Haven, CT 06520-8029. E-mail: stefan.somlo@yale.edu

This article contains supporting information online at www.pnas.org/cgi/content/full/0805062105/DCSupplemental.

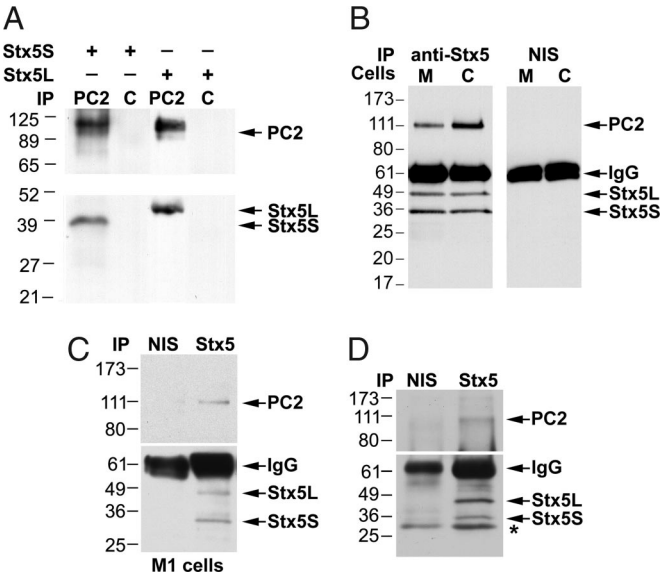

Fig. 1. Interaction of PC2 with both long and short forms of Stx5 in cells and tissue. (*A*) LLC-PK$_1$ cells with stable expression of full-length PC2 were transiently transfected with either Stx5S or Stx5L and immunoprecipitation was performed with anti-PC2 monoclonal antibody YCE2 (PC2) or culture medium (C) as control. The top half was immunoblotted with anti-PC2 polyclonal antisera (YCC2) and the bottom with anti-Stx5 polyclonal antisera. Stx5S and Stx5L coimmunoprecipitate with PC2. (*B*) Native Stx5 coimmunoprecipitation with PC2 from conditionally immortalized mouse kidney cell lines (M and C) made from *Pkd2-BAC* transgenic mice. Cell lysates were immunoprecipitated by using anti-Stx5 antisera or nonimmune rabbit sera (NIS). The top half was immunoblotted with polyclonal anti-PC2 and the bottom with anti-Stx5. (*C*) Native Stx-5 coimmunoprecipitation with PC2 from M1 cells by using the same approach as panel (*B*). (*D*) Native Stx-5 coimmunoprecipitation with PC2 from *Pkd2-BAC* transgenic mouse kidney tissue lysates by using the approach described in (*B*) (*, nonspecific band).

transcript into long (Stx5L) and short (Stx5S) forms based on alternative translation initiation sites (24) (supporting information (SI) Fig. S1*A*). We produced anti-Stx5 antisera by using epitopes in a region of mouse Stx5S (amino acids 55–333) expected to recognize both isoforms of Stx5. The antisera specifically recognize both forms of the protein on immunoblots (Fig. S1 *B* and *C*) and by immunocytochemistry (Fig. S2 *A* and *B*). Interaction of full length PC2 with both isoforms of Stx5 was demonstrated by coimmunoprecipitation from doubly transfected cell lines (Fig. 1 *A*) and both proteins colocalized in ER membranes (Fig. S2*C*). Interaction of the native proteins was initially assessed in conditionally immortalized cell lines isolated from the medullary thick limb (M) and collecting duct (C) segments of a mouse line transgenic for a BAC containing *Pkd2*. The relative expression of PC2 in kidneys from the *Pkd2-BAC* transgenic line is increased approximately fourfold (Fig. S3*A*). Immunopreciptiation of endogenous Stx5 with polyclonal antisera resulted in coimmuprecipitation of PC2 (Fig. 1*B*). In a nontransgenic cell line model, endogenous Stx5 and PC2 were successfully coimmunprecipitated from M1 cells (Fig. 1*C*). Finally, endogenous Stx5 and PC2 were coimmunoprecipitated from whole kidney tissue lysates of the *Pkd2-BAC* transgenic mouse line (Fig. 1*D*). In aggregate, these studies confirm that the interaction discovered in yeast two-hybrid screening occurs in physiological conditions with native full-length proteins.

Direct Interaction of the t-SNARE (H3) Domain of Stx5 and the First 72 aa of PC2. A series of *in vitro* interaction assays using the far Western technique demonstrated direct physical interaction between Stx5 and PC2 and defined the regions of the respective proteins involved in this interaction (Fig. 2). We produced maltose binding protein

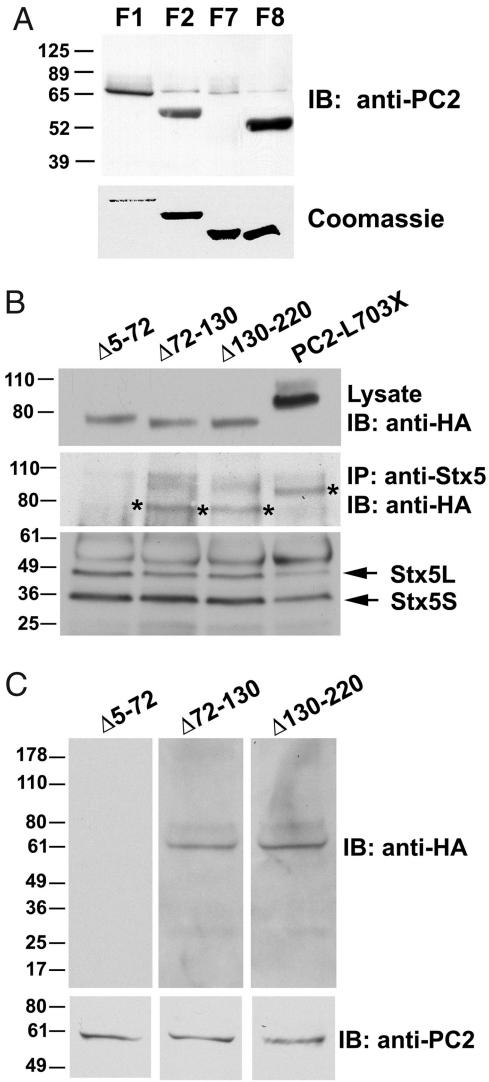

Fig. 2. Stx5 interacts directly with the NH$_2$-terminal 72 aa region of PC2. (*A*) Far Western *in vitro* binding assays mapping the PC2 interaction domain of Stx5. MBP-fusion constructs containing the F1, F2, F7, and F8 portions of Stx5 (see Fig. S1*A*) were expressed, purified, separated by PAGE, and transferred onto PVDF membranes. Purified GST fusion protein containing the cytoplasmic NH$_2$-terminal region of PC2 was incubated with the immobilized Stx5 peptides and specific binding was detected by using an NH$_2$-terminal anti-PC-2 polyclonal antiserum (YCB9, *Top*). F1, F2, and F8 bound PC2; F7 did not. A parallel PVDF membrane was stained with Coomassie blue as an MBP-fusion protein loading control (*Bottom*). (*B*) Coimmunoprecipitation of nested NH$_2$-terminal PC2 constructs with Stx5. PC2-L703X with an intact NH$_2$ terminus and an HA epitope tag and three in-frame deletions of this truncated PC2 (Δ5-72, Δ72-130, and Δ130-220) were stably expressed in LLC-PK$_1$ cells at comparable levels (*Top*) (22). Endogenous Stx5 was immunoprecipitated from lysates of each cell line (*Bottom*). Intact PC2-L703X and deletion forms Δ72-130 and Δ130-220 were successfully coimmunoprecipitated with Stx5, but PC2-L703X deleted for amino acids 5–72 (Δ5-72) did not interact with Stx5 (*Middle*). *, expected migration of PC2-L703X intact and deletion constructs (*Middle*). (*C*) Far Western mapping of the direct interaction between PC2 and Stx5. MBP-fusion protein F1 was expressed, purified, separated by PAGE, and transferred onto PVDF membranes. Parallel blots were incubated with cell lysates from each of three stable cell lines expressing the HA-tagged deletion constructs of PC2-L703X and binding of the latter were detected by anti-HA antisera. The Δ72-130 and Δ130-220 but not the Δ5-72 forms of PC2 showed direct interaction with Stx5 (*Top*). Subsequent far Western blotting with the COOH-terminal anti-PC2 antiserum (YCC2) that does not recognize the COOH-terminal truncated PC2-L703X forms detected directed interaction of endogenous full-length PC2 with Stx5 in all three samples (*Bottom*).

(MBP)-fusion constructs containing the entire cytosolic domain of Stx5S with both syntaxin and t-SNARE domains (F1), a part of the syntaxin domain and all of the t-SNARE domain (F2), only the syntaxin domain (F7), or only the t-SNARE domain (F8) (see Fig. S1*A*). These fusion proteins were expressed in bacteria, purified with amylose binding resin, transferred onto PVDF membranes, and probed with GST-fusion protein containing the NH_2-terminal domain of PC2 used as bait in the yeast two-hybrid screen (amino acids 3–213) (see Fig. 2*A*). PC2 did not bind to the syntaxin proteins Stx1A, Stx4, or Stx12 in the same assay, indicating that the interaction with Stx5 was specific (data not shown) and we excluded the possibility that the GST protein was responsible for the interaction (Fig. S3*B*). PC2 bound to all Stx5 peptides containing the t-SNARE domain but did not bind to the peptide containing only the syntaxin domain (see Fig. 2*A*).

Next, LLC-PK_1 cell lines stably expressing COOH-terminal truncated PC2 (PC2-L703X) or the serial NH_2-terminal deletion constructs Δ(5-72)PC2-L703X, Δ(72-130)PC2-L703X, and Δ(130-220)PC2-L703X (25) were subjected to coimmunoprecipitation studies with anti-Stx5 antisera. All PC2 deletion forms except Δ(5-72)PC2-L703X coimmunoprecipitated with Stx5 (Fig. 2*B*), suggesting the region contained in amino acids 5–72 of PC2 is necessary for interaction with Stx5. The Stx5 interaction region of PC2 is distinct from the RyR interaction domain (12) and the cilia-targeting domain of PC2 (data not shown). The far Western *in vitro* binding assay was used to confirm physical interaction between amino acids 5–72 of PC2 and Stx5. Far Western detection with anti-HA monoclonal antibody showed that Δ(72-130)PC2-L703X and Δ(130-220)PC2-L703X bound to Stx5, but Δ(5-72)PC2-L703X did not (Fig. 2*C*, *Top*). When the far Western binding was performed with anti-PC2 YCC2 on parallel membranes by using the same lysates, binding of native full length PC2 was detected in all three lysates (Fig. 2*C*, *Bottom*). We conclude that amino acids 5–72 of PC2 directly interact with the t-SNARE domain of Stx5.

Stx5 Inhibits Channel Activity of PC2. Coexpression of Stx5 and PC2 did not alter the cellular localization of PC2 by increasing expression in the Golgi or cilia (data not shown). Syntaxin proteins associate with and regulate Ca^{2+} channels [reviewed in (26)]. Given that PC2 is an ER channel that interacts with Stx5, we investigated the role for Stx5 in regulating PC2 channel activity. We had previously defined the single channel properties of over-expressed PC2 in ER-derived vesicles fused to lipid bilayers (5, 11). Addition of increasing concentrations of the F7-MBP fusion protein containing only the syntaxin domain that does not bind PC2 to the cytoplasmic side of the bilayer had no effect on the channel properties of PC2 (Fig. 3 *A*). Addition of the F1-MBP fusion peptide that is capable binding PC2 resulted in concentration dependent inhibition of the channel activity with an IC_{50} of 80 ng/ml (Fig. 3 *B* and *D*). This effect was only observed when F1 was added to the cytoplasmic side of the bilayer, not when it was added to the ER luminal side (data not shown). ER-derived vesicles were also prepared from LLC-PK_1 cells stably over-expressing PC2 with an in-frame deletion of amino acids 5–72 [Δ(5-72)PC2]. The levels of heterologous protein expression in the PC2 and Δ(5-72)PC2 LLC-PK_1 cell lines from which ER vesicles were prepared were comparable (Fig. S4*A*). Fusion of the vesicles to lipid bilayers yielded channel activity typical of the PC2 channel despite the lack of the Stx5 interaction domain (Fig. 3*C*). Addition of increasing concentrations of F1-MBP fusion protein to the cytoplasmic side had no effect on channel activity in bilayers containing Δ(5-72)PC2 (Fig. 3 *C* and *D*). The data show that interaction of Stx5 with PC2 specifically blocks PC2 channel activity by direct interaction and that the first 72 aa of the NH_2 terminus of PC2 are not necessary for channel function but are essential for the inhibition of channel activity by Stx5.

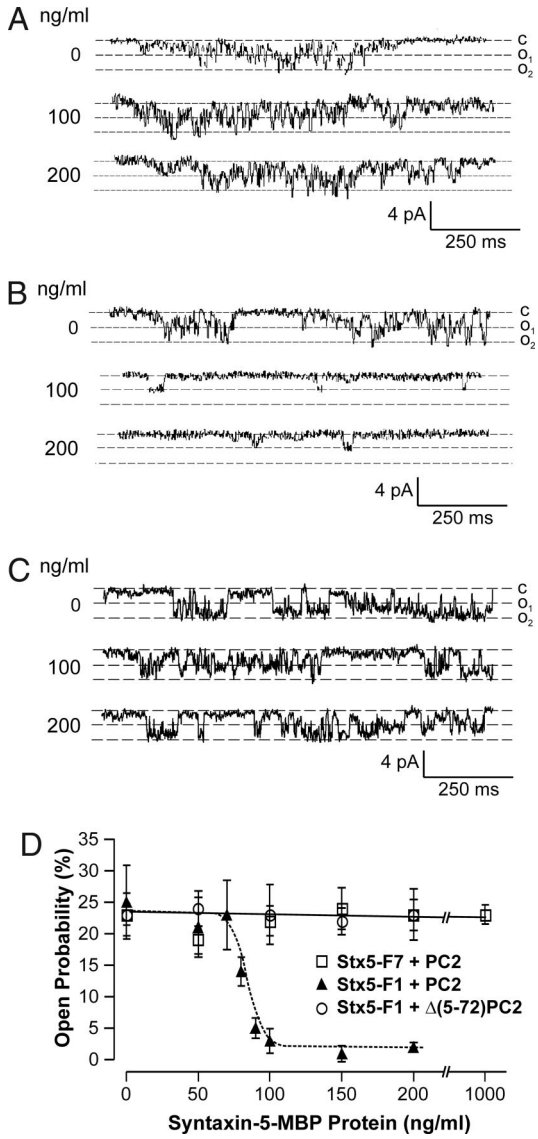

Fig. 3. Binding of Stx5 inhibits the channel activity of PC2. (*A* and *B*) ER-derived vesicles from LLC-PK_1 cells overexpressing full length PC2 were fused to lipid bilayers. Single channel currents generated by PC2 were recorded with 53-mM barium on the ER luminal side as the sole current carrier at a holding potential of 0 mV in the presence of 300-nM free Ca^{2+} on the cytoplasmic side. Channel openings are shown as downward deflections and horizontal lines indicate zero current (C) and successive channel openings (O_1, O_2). Representative channel traces in the presence of increasing concentrations (ng/ml) on the cytoplasmic side of the fusion protein Stx5-F7 containing only the NH_2-terminal coiled coil domain (*A*) and fusion protein Stx5-F1 containing the entire cytosolic domain of Stx5S (*B*) are shown. F1 had no effect on channel activity when added to the ER luminal side (data not shown). (*C*) Representative channel traces when Stx5-F1 is applied to bilayers fused with ER-derived vesicles from LLC-PK_1 cells expressing the Δ(5-72)PC2 construct that cannot bind Stx5, showing that this form of PC2 retains channel activity but Stx5-F1 can no longer block this activity after deletion of the binding domain. (*D*) Summary data of open probabilities for PC2 and Δ(5-72)PC2 over an extended range of Stx5-F7 or Stx5-F1 peptide concentrations in single channel studies under conditions described in (*A*–*C*). The solid line is a theoretical fit for the Stx5-F7 with PC2 (open squares) and Stx5-F1 with Δ(5-72)PC2 (open circles); the dashed curve corresponds to a sigmoid fit for the Stx5-F1 dependence of PC2 open probability with an IC_{50} of 80 ng/ml. Individual points with error bars are the mean ± SEM.

PC2 and Stx5 Regulate Baseline Cytosolic Ca^{2+} Levels and ER Ca^{2+} Content. We have previously shown that over-expression of WT PC2 in LLC-PK_1 cells results in enhanced amplitude and dura-

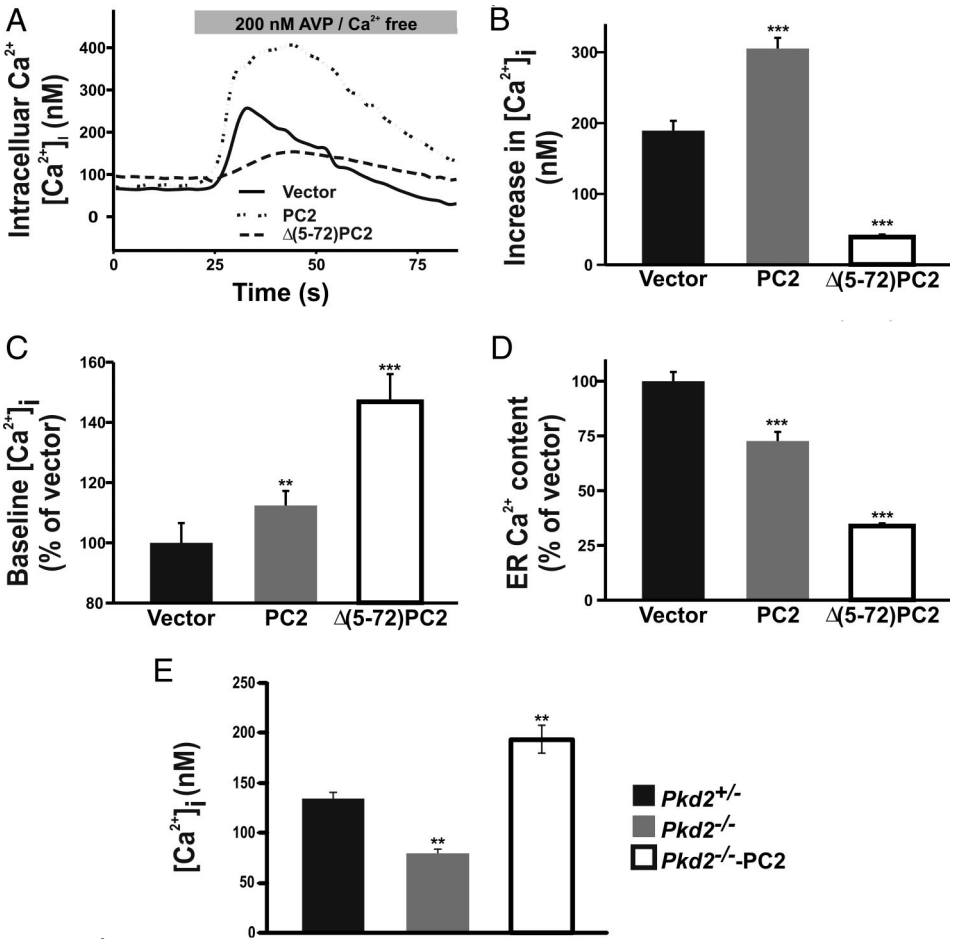

Fig. 4. ER Ca^{2+} channel activity of PC-2 is regulated by Stx5. LLC-PK_1 cells stably expressing empty vector, full length PC2 or Δ(5-72)PC-2 were stimulated with 200nM AVP in the absence of extracellular Ca^{2+}. (*A*) Representative traces during AVP stimulation (gray bar) show the baseline response of vector-expressing cells (solid line) and the increased amplitude and duration of ER Ca^{2+} release in cells over-expressing PC2 (dotted line). The Ca^{2+} response in cells expressing Δ(5-72)PC2 (dashed line) is reduced below the vector-only response. (*B*) Mean amplitude (± SEM) of the peak increase in intracellular Ca^{2+} concentration ($[Ca^{2+}]_i$) above baseline in response to AVP stimulation of LLC-PK_1 cells expressing empty vector, full length PC2 or Δ(5-72)PC2. (*C*) Baseline $[Ca^{2+}]_i$ before AVP stimulation in each of the cell lines expressed as a percentage of Ca^{2+} levels in LLC-PK_1 cells expressing only empty vector. (*D*) ER Ca^{2+} content expressed as a percent of ER content in cells expressing only empty vector. (*E*) Basal $[Ca^{2+}]_i$ in *Pkd2*$^{+/-}$ ($n = 104$), *Pkd2*$^{-/-}$ ($n = 109$) and *Pkd2*$^{-/-}$ PC2 cells ($n = 83$) re-expressing PC2 on a null background. ***, $P < 0.001$; **, $P < 0.01$.

tion of AVP-induced Ca^{2+} release from intracellular pools (5, 11). Given the regulation of PC2 channel activity by Stx5 in single channel studies, we assessed whether interaction with Stx5 had an effect on PC2-dependent intracellular Ca^{2+} homeostasis *in vivo*. We used ratiometric Ca^{2+} imaging to monitor changes in cytosolic and ER Ca^{2+} content in LLC-PK_1 cells stably expressing empty vector, full-length PC2, or Δ(5-72)PC2. Protein expression levels for two independent stable cell line clones for each were similar and > 90% of cells expressed either PC2 or Δ(5-72)PC2 in the respective cell lines (Fig. S4). All cell lines responded with increases in cytosolic Ca^{2+} ($[Ca^{2+}]_i$) on treatment with 200-nM AVP in the absence of extracellular Ca^{2+} (Fig. 4*A*).

The mean peak rise of $[Ca^{2+}]_i$ in response to AVP stimulation was 189 nM in cells expressing the empty vector ($n = 176$) and 309 nM in cells over-expressing full length PC2 ($n = 191$) (Fig. 4 *A* and *B*) (5). However, cells expressing Δ(5-72)PC2 ($n = 219$) showed only a 39-nM increase in $[Ca^{2+}]_i$ response to AVP (Fig. 4 *A* and *B*). The mean baseline $[Ca^{2+}]_i$ in unstimulated LLC-PK_1 cell lines expressing empty vector, PC2 and Δ (5-72)PC2 was 69 ± 4.5 nM, 77 ± 3.3 nM ($P < 0.01$), and 101 ± 6.3 nM ($P < 0.001$), respectively. Expressed as a percent of the empty vector baseline $[Ca^{2+}]_i$, PC2 over-expressing cells had a resting Ca^{2+} ≈12% above control, whereas cells expressing Δ(5-72)PC2 had resting Ca^{2+} ≈47% above baseline (Fig. 4*C*). This increase in cellular $[Ca^{2+}]_i$ showed an inverse correlation to ER Ca^{2+} stores which were reduced to ≈73% of baseline in cells over-expressing WT PC2 and to ≈34% in cells expressing Δ(5-72)PC2 (Fig. 4*D*). LLC-PK_1 cells expressing Δ(5-72)PC2 that does not bind Stx5 have elevated resting baseline cellular $[Ca^{2+}]_i$, reduced ER Ca^{2+} content, and a minimal increase in $[Ca^{2+}]_i$ after stimulation with AVP. The diminished ER Ca^{2+} release in Δ(5-72)PC2 cells in response to AVP reflects an antecedent depletion of ER Ca^{2+} stores and consequent rise in cellular baseline $[Ca^{2+}]_i$ because of loss of inhibition of the ER PC2 channel when PC2 cannot bind Stx5.

To test whether endogenous PC2 functions in a similar manner to over-expressed PC2 in determining cellular Ca^{2+} homeostasis in epithelial cells, we used our previously described paired *Pkd2*$^{+/-}$ and *Pkd2*$^{-/-}$ cells derived from mutant mice (Fig. 4*E*) (25). *Pkd2*$^{+/-}$ cells ($n = 104$) had mean $[Ca^{2+}]_i$ of 134 ± 6 nM. In the absence of PC2, *Pkd2*$^{-/-}$ cells ($n = 109$) had markedly reduced $[Ca^{2+}]_i$ of 80 ± 4 nM; heterologous re-expression of PC2 in the *Pkd2*$^{-/-}$ cells ($n = 83$) results in increased $[Ca^{2+}]_i$ to 193 ± 14 nM (see Fig. 4*E*). In aggregate, the data suggest that resting $[Ca^{2+}]_i$ in epithelial cells depend on PC2 activity, which in turn depends on both PC2 expression level and on inhibition of the PC2 channel by physical interaction with Stx5.

Discussion

We used an unbiased protein interaction screen to discover Stx5, an ER and Golgi-associated t-SNARE (22, 23), as a PC2 NH_2-

terminal interacting partner. Before this, RyR was the only known PC2 NH_2-terminus-binding partner (12). However, even in the latter, the functional interaction inhibiting RyR function is mediated by the COOH-terminal tail of PC2 (12). The only previously known functional domain in the intracellular NH_2-terminal region of PC2 is the cilial-targeting signal R_6VxP (25). Stx5 and PC2 are expressed and functional in the ER, so the cellular location for the two proteins is permissive for a physiological interaction. Stx5 interacts with PC2 via its t-SNARE domain (also known as the H3 domain) located in the COOH-terminal third of the molecule before the transmembrane domain. This same domain in Stx1A is responsible for its interaction with voltage-dependent Ca^{2+} channels (VDCC) (27), Kv channels (28), ENaC (21), and CFTR (29). Stx1A interaction with ENaC and CFTR affects cell surface expression of the respective channels (30), but we were not able to identify any changes in the cellular location of PC2 with coexpression of Stx5. Direct physical interaction of PC2 and Stx5 was shown with *in vitro* binding assays, and the association of native proteins in cells and tissues was demonstrated by coimmunoprecipitation studies. The specificity of the Stx5 interaction was suggested by the failure of several other syntaxins to interact with PC2 in our assays. Binding of Stx1A to VDCC, Kv, EnaC, and CFTR inhibits transport activity of each channel (18–21). In keeping with this paradigm, the interaction of Stx5 with PC2 inhibits the PC2 channel.

Ca^{2+} regulates SNARE complex activity (31) and PC2 is the only Ca^{2+} channel beside the synaptic *N*- and P/Q-type VDDCs known to be gated by a syntaxin. In the case of the VDCCs, the association of the t-SNARE with the Ca^{2+} channel has direct functional implications (27). Synaptic exocytic events are dependent on relatively high Ca^{2+} concentrations that alter the SNARE complex structure to regulate membrane fusion and neurotransmitter release (31). The high Ca^{2+} concentrations required for this process are best achieved in the immediate proximity of the channel proteins (27), suggesting that the physical association with VDCC is permissive for SNARE complex assembly and function. Depending on the stage in the exocytic cycle, the interacting Stx1A may contribute to VDCC inactivation, providing feedback to modulate Ca^{2+} entry (27). PC2 may serve an analogous role in ER-to-Golgi SNARE complex function, as VDCC serve in presynaptic vesicle fusion. The association of Stx5 with PC2 may allow for local elevations in Ca^{2+} sufficient to cause SNARE complex assembly and function in the ER-to-Golgi compartment.

There is evidence that PC2 can function independently of PC1 in various stages of development and in different cellular locations. For example, *Pkd2*$^{-/-}$ mice have defects in left-right axis determination (32), whereas *Pkd1*$^{-/-}$ mice do not (33), suggesting that PC2 and PC1 functions diverge in embryonic nodal cilia. In lumen-forming epithelial cells, PC2 and PC1 colocalize in cilia (2, 3), but PC2 is also abundantly expressed in the ER (4) and PC1 does not appear to be (Y. Cai, S.S., unpublished observations). Another interacting proteins know to inhibit the PC2 channel is mDia, a downstream effector of RhoA that binds to the COOH terminus of PC2 (15, 34). mDia is involved in actin dynamics, is not associated with the ER membrane (17), and is unlikely to modulate PC2 activity in the ER.

Our data suggest that abundant ER PC2 has a role in Ca^{2+} homeostasis in epithelial cells. There is a graded change in cytosolic Ca^{2+} concentration with absence, haploinsufficiency, and over-expression of PC2, respectively. This suggests that the level of PC2 expression in the setting of a presumed constant level of Stx5 results in altered cytosolic Ca^{2+} levels. As a corollary, patients carrying heterozygous *PKD2* mutations will have a reduction in resting steady-state cellular Ca^{2+} levels. Similar findings have been reported in smooth muscle cells from *Pkd2*$^{+/-}$ mice (35). The critical role of Stx5 in PC2-dependent epithelial cell Ca^{2+} homeostasis is shown by the significant depletion of ER stores and the increase in cytosolic Ca^{2+} when the interaction of Stx5 with functional PC2 channels is abolished. Mutations in RyR that cause exercise-induced sudden cardiac death result from "leaky" RyR channels because of decreased binding to the calstabin-2 subunit that normally stabilizes the closed state of the RyR channel (36). PC2 is expressed in cardiac muscle where it regulates RyR (12); it may be that independent of this function, mutations in the Stx5 binding domain of PC2 that reduce Stx5 binding may predispose individuals to cardiac arrhythmias under certain conditions. Conversely, to the extent that PC2-dependent cellular Ca^{2+} is important to the alterations of cellular phenotypes that result in cyst formation *in vivo*, agents that selectively diminish the Stx5-PC2 interaction may be useful in modulating cellular Ca^{2+} in ADPKD resulting from loss of PC1.

Finally, changes in total cellular Ca^{2+} in response to laminar shear stress under flow have been attributed to the PC1-PC2 complex in ciliated epithelial cell monolayers (8, 9, 37). The rise in cellular Ca^{2+} requires both Ca^{2+} entry and Ca^{2+} release from ER stores. The relative contribution from these sources to the rise in total cellular Ca^{2+} is uncertain, although it is unlikely that the bulk of the Ca^{2+} enters exclusively through the ciliary channels. $InsP_3R$ and RyR have been implicated in the release of ER stores in response to flow (8, 9), but the role of PC2 has not been evaluated. This is especially noteworthy, because PC2 has been implicated in both $InsP_3R$ and RyR function (6, 12). The role of PC2 in epithelial cellular Ca^{2+} homeostasis described in the current study suggests that the ER-release channel function of PC2 needs to be directly evaluated in both the cell culture-based and *in vivo* models to fully understand the role of PC2 and cellular Ca^{2+} levels in the pathogenesis of polycystic kidney disease.

Materials and Methods

Yeast Two-Hybrid Screening. Two-hybrid screening was performed by the method described in the literature (38, 39). Briefly, a LexA-fusion protein bait containing codons 3 to 213 of PC2 in the pBTM116 vector was used to screen a mouse embryo days 9 to 11, library cloned into pVP16 as prey. Bait and prey were cotransformed into L40 strain cells and clones that grew in the absence of His, Trp, and Leu were confirmed by using a β-gal filter assay (39). Positive clones were cured of the pBTM116 LexA-PC2 plasmid by growth in Trp-containing medium and then mated against yeast strain NA87–11A, containing plasmid pBTM116 expressing either LexA-PC2 (positive control) or LexA fusion proteins with portions of the CD40 cytosolic domain or lamin C (39). Mated cells were selected in medium that lacked Trp (pBTM116 plasmid) and Leu (pVP16 plasmid) and specificity of interaction confirmed by the ability to transactivate a *lacZ* reporter gene by using the β-gal filter assay. Confirmed clone inserts were amplified by PCR and identified by sequencing. Stx5 was one of 36 interacting sequences identified in this screen.

Expression Constructs. The PC2 constructs have been previously described (4, 25). Stx5 cDNA was amplified by RT-PCR from mouse brain polyA RNA (Clontech) by using SuperScript II (Invitrogen) with the following primers: 5′-ggaattc ATG TTC TGC CGG GAT CGG-3′ and 5′-acgcgtcgac TCA GGC AAG GAA GAC CAC AAA G-3′. Products were subcloned into pCDNA3.1/myc (Invitrogen) and sequenced in both directions. Partial Stx5 clones to express fusion proteins were produced by PCR, subcloned into pMAL-C2 vector, sequence verified, and purified by amylose-resin chromatography (NEB).

Antibodies and Immunofluorescent Labeling. Immunofluorescent cell labeling was performed as previously described (25). Rabbit polyclonal antisera (HRP) were generated against the F1-PGEX2T fusion peptide containing the cytoplasmic domain of mouse Stx5. The following primary antisera/antibodies were used in this study: polyclonal antihuman PC2, YCC2 (C-terminal), and YCB9 (N-terminal) (4); mouse monoclonal antihuman PC2, YCE2 (C-terminal) (11); polyclonal anti-HA (71–5500, Zymed); monoclonal anti-HA (mouse, MMS-101R, Covance; rat, clone 3F10, Roche); mouse monoclonal anti-Myc ab (clone 9E10, Roche).

Cell Lines. LLC-PK_1 (CRL1392, ATCC) and M1 (kind gift from Eero Lehtonen, University of Helsinki, Helsinki, Finland) cells were maintained in DMEM:F12 (1:1) with 5% FBS. *Pkd2*$^{-/-}$ cell lines (2D2, 5C1) and *Pkd2*$^{+/-}$ cell lines (3B3, 2G10) have been described previously (25). Full-length PC2 was re-expressed in 2D2 cells. Conditionally immortalized (Immortomouse, Charles River) cell lines from *Pkd2*

BAC transgenic lines were maintained in defined medium as described previously (25). At least two independent cell lines were used in all experiments to control for clonal artifacts.

***In Vitro* Binding Assays.** For fusion protein *in vitro* binding, purified pMAL-Stx5 fusion peptides F1, F2, F7, and F8 (see Fig. S1) were transferred onto PVDF membranes. Ten μg of purified GST-PC2 NH_2-terminal fusion protein (amino acids 3–213) (4) was diluted in 10-ml reaction buffer (10-mM Tris, pH 7.5; 1-mM EDTA; 1% CHAPS; 0.1% Nonidet P-40, and protease inhibitors) and incubated with PVDF membranes at 4°C for 2 h. After washing with three exchanges of reaction buffer, the bound GST-PC2 was detected by using NH_2-terminal anti-PC2 antisera (YCB9) (1:2,000) (4). For native protein *in vitro* binding, 500 μg of protein from total cell lysates of LLC-PK_1 cells stably expressing HA epitope-tagged PC2 NH_2-terminal deletion constructs Δ(5-72)PC2-L703X, Δ(72-130)PC2-L703X and Δ(130-220)PC2-L703X were each suspended in 10-ml reaction buffer and incubated with PVDF membranes containing immobilized Stx5 pMAL-F1 fusion protein at 4°C for 2 h. The binding of the NH_2-terminal deletion constructs on the membranes were detected with anti-HA and binding of native PC2 was detected with YCC2 (1:6,000).

Immunoprecipitation and Immunoblotting. Cells were lysed with 1% CHAPS in 10-mM Tris, pH 7.5, 1-mM EDTA, and protease inhibitors (lysis buffer). Immunoprecipitation from the lysates was performed with either anti-PC2 or anti-Stx5 primary antisera/antibodies, and presence of the respective binding partner in the immunoprecipitates was monitored by immunoblotting by using specific antisera followed by detection with ECL (Amersham).

Bilayer Recordings and Ratiometric Ca^{2+} Imaging. Bilayer recordings were performed as previously described (5, 11). The methods are described in the SI *Methods*. The ratiometric Ca^{2+} imaging methods have also been previously described (40). Briefly, LLC-PK_1 cell lines were grown on glass coverslips to subconfluent density. Cells were loaded with 5-μM Fura-2/AM at 37°C for 30 min in a standard solution (in mM): 137 NaCl, 5 KCl, 1 $MgSO_4$, 1 Na_2HPO_4, 2 $CaCl_2$, 10 Hepes, 5.6 glucose, pH 7.4, 0.02% pluronic acid, and 1 mM probenecid. After loading, Fura-2 was allowed to de-esterify for at least 10 min at room temperature in standard solution. Coverslips were mounted in a perfusion chamber and placed on an inverted Zeiss Axiovert 135 stage. Fluorescence data were acquired on a PC running Imaging Workbench software (INDEC Biosystems) via a CCD camera (SensiCam, ASI). For AVP stimulation experiments, cells were perfused with 200-nM AVP in Ca^{2+}-free Hepes buffer (in mM): 130 NaCl, 4.7 KCl, 2.3 $MgSO_4$, 1.2 KH_2PO_4, 10 EGTA, 20 Hepes, 5 glucose, pH 7.4.

Intracellular free Ca^{2+} concentration ($[Ca^{2+}]_i$) was derived from background subtracted F340/F380 fluorescent ratios (R) after *in situ* calibration (38, 39) according to the following equation: $[Ca^{2+}]_i$ (nM) = K_d*Q*($R-R_{min}$)/($R_{max}-R$), where K_d is the dissociation constant of fura-2 for Ca^{2+} at room temperature (i.e., 225 nM); Q is the fluorescence ratio of the emission intensity excited by 380 nm in the absence of Ca^{2+} to that during the presence of saturating Ca^{2+}; R_{min} and R_{max} are the minimal or maximal fluorescence ratios respectively. R_{min} was measured by perfusion with Ca^{2+}-free Hepes buffer (as described above) containing 10-μM ionomycin. R_{max} was obtained by perfusion with standard solution containing 10-mM $CaCl_2$ and 10-μM ionomycin. ER-Ca^{2+} was measured by depletion of ER-stores with 5 μM of the sarco-endoplasmic reticlum Ca ATPase inhibitor thapsigargin over 5 min in Ca^{2+}-free Hepes buffer. Released Ca^{2+} was calculated by subtracting baseline Ca^{2+} and plotted over time. The area under the release curve was calculated by using a macro in SigmaPlot 10 (Systat Software).

Statistics. Comparisons of cellular responses were carried out by using one-way analysis of variance on ranks (the nonparametric Kruskal-Wallis test) with post-test multiple pair-wise comparisons done by Dunn's method.

ACKNOWLEDGMENTS. We thank Takaaki Sato for help with the yeast two-hybrid system and Jeff Sfakianos and Ira Mellman for valuable insights. This work was supported by the National Institutes of Health/National Institute of Diabetes and Digestive and Kidney Diseases Grant DK54053 (to S.S.) and Grant DK57328 (to S.S. and B.E.E.); a grant from the National Kidney Foundation (Y.M.); a Polycyctic Kidney Disease Foundation Grant 20a2r (to L.G.); a grant from the German National Merit Foundation (W.B. and C.C.); and a National Institutes of Health predoctoral fellowship (G.I.A.). The authors are members of the Yale Center for the Study of Polycystic Kidney Disease (P50 DK57328).

1. Somlo S, Torres VE, Caplan MJ (2007) in *Seldin and Giebisch's The Kidney: Physiology & Pathophysiology*, eds. Alpern RJ, Hebert SC (Academic, San Diego, CA) pp. 2283–2314.
2. Pazour GJ, San Agustin JT, Follit JA, Rosenbaum JL, Witman GB (2002) Polycystin-2 localizes to kidney cilia and the ciliary level is elevated in orpk mice with polycystic kidney disease. *Curr Biol* 12:R378–R380.
3. Yoder BK, Hou X, Guay-Woodford LM (2002) The polycystic kidney disease proteins, polycystin-1, polycystin-2, polaris, and cystin, are co-localized in renal cilia. *J Am Soc Nephrol* 13:2508–2516.
4. Cai Y, *et al.* (1999) Identification and characterization of polycystin-2, the PKD2 gene product. *J Biol Chem* 274:28557–28565.
5. Koulen P, *et al.* (2002) Polycystin-2 is an intracellular calcium release channel. *Nat Cell Biol* 4:191–197.
6. Li Y, Wright JM, Qian F, Germino GG, Guggino WB (2005) Polycystin 2 interacts with type I inositol 1,4,5-trisphosphate receptor to modulate intracellular Ca2+ signaling. *J Biol Chem* 280:41298–41306.
7. Praetorius HA, Spring KR (2003) Removal of the MDCK cell primary cilium abolishes flow sensing. *J Membr Biol* 191:69–76.
8. Nauli SM, *et al.* (2003) Polycystins 1 and 2 mediate mechanosensation in the primary cilium of kidney cells. Nat Genet 33:129–137.
9. Praetorius HA, Spring KR (2001) Bending the MDCK cell primary cilium increases intracellular calcium. *J Membr Biol* 184:71–79.
10. Nilius B, Voets T, Peters J (2005) TRP channels in disease. *Sci STKE* 2005:re8.
11. Cai Y, *et al.* (2004) Calcium dependence of polycystin-2 channel activity is modulated by phosphorylation at Ser812. J Biol Chem 279:19987–19995.
12. Anyatonwu GI, Estrada M, Tian X, Somlo S, Ehrlich BE (2007) Regulation of ryanodine receptor-dependent calcium signaling by polycystin-2. *Proc Natl Acad Sci USA* 104:6454–6459.
13. Xu GM, *et al.* (2003) Polycystin-1 activates and stabilizes the polycystin-2 channel. *J Biol Chem* 278:1457–1462.
14. Li Q, *et al.* (2005) Alpha-actinin associates with polycystin-2 and regulates its channel activity. *Hum Mol Genet* 14:1587–1603.
15. Bai CX, *et al.* (2008) Activation of TRPP2 through mDia1-dependent voltage gating. *EMBO J* 27:1345–1356.
16. Wu Y, *et al.* (2006) Kinesin-2 mediates physical and functional interactions between polycystin-2 and fibrocystin. *Hum Mol Genet* 15:3280–3292.
17. Brandt DT, *et al.* (2007) Dia1 and IQGAP1 interact in cell migration and phagocytic cup formation. *J Cell Biol* 178:193–200.
18. Bezprozvanny I, Scheller RH, Tsien RW (1995) Functional impact of syntaxin on gating of N-type and Q-type calcium channels. *Nature* 378:623–626.
19. Fili O, *et al.* (2001) Direct interaction of a brain voltage-gated K+ channel with syntaxin 1A: functional impact on channel gating. *J Neurosci* 21:1964–1974.
20. Naren AP, *et al.*(1997) Regulation of CFTR chloride channels by syntaxin and Munc18 isoforms. *Nature* 390:302–305.
21. Condliffe SB, Carattino MD, Frizzell RA, Zhang H (2003) Syntaxin 1A regulates ENaC via domain-specific interactions. *J Biol Chem* 278:12796–12804.
22. Rowe T, Dascher C, Bannykh S, Plutner H, Balch WE (1998) Role of vesicle-associated syntaxin 5 in the assembly of pre-Golgi intermediates. *Science* 279:696–700.
23. Hay JC, *et al.* (1998) Localization, dynamics, and protein interactions reveal distinct roles for ER and Golgi SNAREs. *J Cell Biol* 141:1489–1502.
24. Hui N, *et al.* (1997) An isoform of the Golgi t-SNARE, syntaxin 5, with an endoplasmic reticulum retrieval signal. *Mol Biol Cell* 8:1777–1787.
25. Geng L, *et al.* (2006) Polycystin-2 traffics to cilia independently of polycystin-1 by using an N-terminal RVxP motif. *J Cell Sci* 119:1383–1395.
26. Atlas D (2001) Functional and physical coupling of voltage-sensitive calcium channels with exocytotic proteins: ramifications for the secretion mechanism. *J Neurochem* 77:972–985.
27. Catterall WA (1999) Interactions of presynaptic Ca2+ channels and snare proteins in neurotransmitter release. *Ann N Y Acad Sci* 868:144–159.
28. Yamakawa T, *et al.* (2007) Interaction of syntaxin 1A with the N-terminus of Kv4.2 modulates channel surface expression and gating. *Biochemistry* 46:10942–10949.
29. Naren AP, Quick MW, Collawn JF, Nelson DJ, Kirk KL (1998) Syntaxin 1A inhibits CFTR chloride channels by means of domain-specific protein-protein interactions. *Proc Natl Acad Sci USA* 95:10972–10977.
30. Saxena S, Quick MW, Warnock DG (2000) Interaction of syntaxins with epithelial ion channels. *Curr Opin Nephrol Hypertens* 9:523–527.
31. Bhalla A, Chicka MC, Tucker WC, Chapman ER (2006) Ca(2+)-synaptotagmin directly regulates t-SNARE function during reconstituted membrane fusion. *Nat Struct Mol Biol* 13:323–330.
32. Pennekamp P, *et al.* (2002) The ion channel polycystin-2 is required for left-right axis determination in mice. *Curr Biol* 12:938–943.
33. Karcher C, *et al.* (2005) Lack of a laterality phenotype in Pkd1 knock-out embryos correlates with absence of polycystin-1 in nodal cilia. *Differentiation* 73:425–432.
34. Rundle DR, Gorbsky G, Tsiokas L (2004) PKD2 interacts and co-localizes with mDia1 to mitotic spindles of dividing cells: role of mDia1 IN PKD2 localization to mitotic spindles. *J Biol Chem* 279:29728–29739.
35. Qian Q, *et al.* (2003) Pkd2 haploinsufficiency alters intracellular calcium regulation in vascular smooth muscle cells. *Hum Mol Genet* 12:1875–1880.
36. Lehnart SE, *et al.* (2008) Leaky Ca release channel/ryanodine receptor 2 causes seizures and sudden cardiac death in mice *J Clin Invest* 118:2230–2245.
37. Praetorius HA, Spring KR (2003) The renal cell primary cilium functions as a flow sensor. *Curr Opin Nephrol Hypertens* 12:517–520.
38. Vojtek AB, Hollenberg SM, Cooper JA (1993) Mammalian Ras interacts directly with the serine/threonine kinase Raf. *Cell* 74:205–214.
39. Sato T, Irie S, Krajewski S, Reed JC (1994) Cloning and sequencing of a cDNA encoding the rat Bcl-2 protein. *Gene* 140:291–292.
40. Boehmerle W, *et al.* (2007) Chronic exposure to paclitaxel diminishes phosphoinositide signaling by calpain-mediated neuronal calcium sensor-1 degradation. *Proc Natl Acad Sci USA* 104:11103–11108.